Advanced Composite Materials

ISSN: 0924-3046 (Print) 1568-5519 (Online) Journal homepage: http://www.tandfonline.com/loi/tacm20

Optimization of gradient effects on the compressive properties of silica-reinforced rubber composite

Dong-Joo Lee & Sang-Ryeoul Ryu

To cite this article: Dong-Joo Lee & Sang-Ryeoul Ryu (2015) Optimization of gradient effects on the compressive properties of silica-reinforced rubber composite, Advanced Composite Materials, 24:5, 481-494, DOI: 10.1080/09243046.2014.964987

To link to this article: http://dx.doi.org/10.1080/09243046.2014.964987

Advanced Composite Materials, 2015
Vol. 24, No. 5, 481–494, http://dx.doi.org/10.1080/09243046.2014.964987

Optimization of gradient effects on the compressive properties of silica-reinforced rubber composite

Dong-Joo Lee* and Sang-Ryeoul Ryu

School of Mechanical Engineering, Yeungnam University, Gyungsan, Gyungbuk, 712-749, Korea

(*Received 13 May 2014; accepted 10 September 2014*)

The gradient effects depending on the manufacturing conditions, such as the rotating speed (rpm) and time (h), silica particle size and interfacial treatments on the compressive properties of silica-reinforced rubber composites were examined. Based on the experimental results, the window of the best manufacturing conditions to obtain the maximum compressive properties was investigated. By developing a simple model, the optimal gradient pattern of the silica distribution was proposed. The degree of the distribution gradient (D_g) should be maximized to have the best compressive properties. A higher D_g could be obtained by increasing the rotating speed and time. On the other hand, the highest D_g has the problem of popping out the silica located in the surface during compressive loading, even in early stages. To overcome the model-predicted ideal pattern of silica particles, the distribution pattern for modified experimental observations can be obtained by changing the curing processes. In addition, the surface treatments of silica significantly affect the manufacturing conditions due to a higher adsorption capacity of rubber molecules that interfere with silica movement by the centrifugal force.

Keywords: FGM; silicone rubber; compressive modulus; distribution gradient; silica

1. Introduction

Functionally graded materials (FGMs) attract increasing attention in many engineering applications because of the increasing performance demands and tailorable reinforcement capabilities of their various properties. In general, FGMs contain either a gradual or a stepwise change in material properties along a given direction. In particulate composites, a graded structure can be obtained by either changing the particle volume fraction or the particle size along the thickness of the composite.[1,2] Functionally graded metal and ceramic composites have been studied widely, fabricated, and characterized.[3,4] On the other hand, relatively few studies have examined polymeric materials even though there are many advantages such as optical properties, thermal stress relaxation, and mechanical properties for gradient polymer. In particular, FGM with an elastomeric matrix has not been widely studied even though there are many advantages, because rubber is used under a compressive load in many applications such as tires, shock absorbers, and dampers. The gradient effects of FGMs can be more significant under compressive loads than tensile loads for an elastomeric material with short or particulate fillers due to the failure mechanisms.[5,6]

*Corresponding author. Email: djlee@yu.ac.kr

Among many fabrication methods, applying a centrifugal force is considered the most economical and attractive process. Centrifugation has been used to produce a graded distribution of carbon fiber [7] and graphite, in an epoxy resin matrix [8,9] and in polymer matrix-based FGMs. The performance of FGMs depends on the concentration profile and uniform dispersion in the matrix. In addition, epoxy-based composites have been fabricated with different fillers [10,11], and other matrix such as polyurethane [12] was also studied. In these studies, the FGMs have improved mechanical properties compared with their homogeneous counterparts. On the other hand, an improvement in mechanical properties is achieved at the expense of dimensional stability at various temperature and moisture conditions.

Recently, silica has attracted considering attention due to the alternative non-black reinforcing filler that can be used widely to produce colored rubber products with excellent tear strength, high abrasion resistance, and low rolling resistance.[13] In addition, with increasing demand for the control of vibrations and noise, the importance of developing damping materials with silica is becoming vital in many industries.[14] Silica, however, is less compatible with some elastomers and it is not easy to disperse small-sized silica. To maximize the potential of silica as a reinforcing filler and expand the applications of the elastomers, the development and optimizing of FGMs is critical.[15] Therefore, FGMs with an elastomeric matrix can be a good candidate material for these applications with a controllable size, shape and filler content, and distribution.

To maximize the use of FGM, the key issue lies in determining the optimum spatial dependence for the composition and in predicting the characteristics of an FGM for a given composition profile during fabrication and under in-service conditions. Therefore, a simple model for design, processing, and performance is needed. There are numerous studies to establish the FGM behaviors. [16,17] However, many of these studies are limited to a specific application and are not easy to use. Furthermore, there is very limited study for elastomeric composites.

The aim of this study was to examine the compressive properties of silica-reinforced gradient rubber composite depending on the manufacturing conditions, such as the rotating speed (rpm), time (h), silica particle size, and interfacial treatments. In addition, the optimized pattern of the particle distribution was determined based on the simple analytical model. Also, the degree of the gradient is simplified to predict the effects of distribution gradient. The curing process was modified to obtain the best distribution pattern that gave significantly improved mechanical properties.

2. Experimental

The matrix material used in this study was room temperature vulcanization (RTV) silicone rubber (Shinetsu, KE-12), and the reinforcing filler was silica with a particle size ranging from 30 to 340 μm and a volume content ranging from 0 to 40 phr. The particle size is measured using a laser diffraction particle size analyzer (LS 13 320, Beckman Coulter Inc. US) and ethanol as a solvent. Figure 1 shows the typical particle size distribution of the used silica with a mean diameter of 30 μm (the actual value: 26.6 μm).

After mixing the matrix with the silica fillers, the mixture was placed in vacuum for 5 min. Then, a hardener (CAT-RM) of 0.5 phr was added and placed again in vacuum for 5 min. The final compound was poured into the mold and placed in a vacuum for another 5 min. By considering the working (30 min) and curing (8 h) time of the matrix, the rotating time was 0, 0.5, 1, and 2 h; the rotating speed was 0, 210, 400,

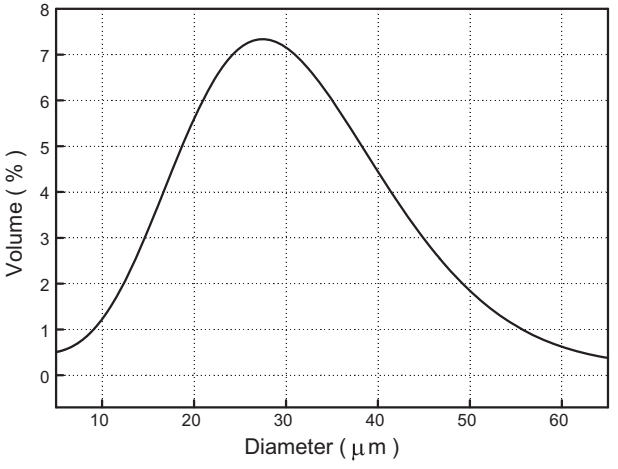

Figure 1. The size distribution of used silica with the mean diameter of 30 μm.

and 560 rpm. In addition, the temperature of the mold was increased up to 50 °C for rapid curing in the mold surface during rotation, to prevent the silica from being located at the surface. If located extremely at the surface, the particles can protrude easily during compressive deformation. To investigate the particle distribution within the specimen, the specific gravity of different locations is measured using the electronic densimeter (Type DH-202, Densicom Inc. Korea).

The silica surface was treated by atmospheric pressure flame plasma (APFP, Super Flame Center 100®, API Inc. Korea). The distance between the burner port and silica was 40 mm, the velocity was 30 m/min, and the sample was treated reciprocally four times.[5,6]

The specimen was a cylinder type with 40 mm in height and 25 mm in diameter. A compressive test was performed using a Shimatzu machine (AG-5000E) with a constant velocity of 5 mm/min. The compressive modulus is measured between the strain of $\varepsilon = 0.1$ and $\varepsilon = 0.2$ for the specimen. All data reported are the mean of more than five specimens.

3. Results and discussion

Three different sizes of silica with 40 phr and three different rotating velocities were initially chosen to understand the silica distribution, volume fraction, and size of silica under a centrifugal force. Figure 2 shows the effects of the particle size on the compressive modulus after 1 h at 400 rpm. As the particle size increased from 30 to 340 μm, the compressive modulus increased from 2.73 to 3.52 MPa, at a rotating velocity of 400 rpm for 1 h. As expected, when the particle size decreased, there was a decrease in the compositional gradients that lead to a small increase in compressive modulus for a given period. On the other hand, this trend of increasing the modulus with the particle size is the same for different volume contents and rotating velocities, even though the increasing rate was different. In this study, the size variations as shown in Figure 1 are not considered since these size distribution of used silica is quite similar for all sizes. However, the particle distribution depending on the particle size and location should be examined carefully in a future experiment.

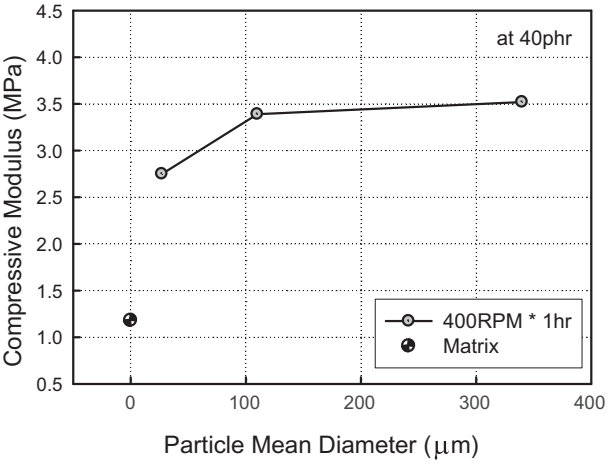

Figure 2. Effect of the particle mean diameter on the compressive modulus of the composites.

Figure 3 shows the effects of the rotating velocity and particle volume content on the compressive modulus. The gradient effects became more significant with increasing volume content. In addition, there should be optimal condition depending on the particle size, volume, and rotating conditions, such as the velocity and time, because the modulus decreases at 560 rpm for 1 h. For the specimen with 40phr, the maximum modulus reaches at 400 rpm; the specimen with 25 phr shows the maximum modulus at 210 rpm, even though the modulus was quite low. It is believed that the compound with a low V_p has a low viscosity and can have an easy alignment at a lower speed.

Figure 4 shows the compressive modulus with 110 μm and 40 phr as functions of the RPM and rotation time. In general, the compressive modulus increases gradually with increasing RPM and rotation time up to a certain condition and then decreases. It closes to the maximum at 300 rpm at 2 h and 400 rpm for 1 h, and decreases slowly thereafter. However, it keeps increasing with the specimen for 0.5 h rotation up to 560 rpm, which is the limit for experimental setup in this study. Generally, it can be expected that the rotating speed and time have a reciprocal relationship. If one of them is excessive, the compressive modulus deceases because the filler tends to be located extremely in the edge of the specimens and pop out during the compressive loading. The compressive strength also has a similar trend.

Figure 5 shows the effects of the plasma treatment on silica (110 μm) on the compressive modulus as a function of the rotation time. Compared to the untreated specimen which shows the maximum modulus at 1 h with 400 rpm, the modulus of the specimen with the APFP treatment shows a rapid increase even at 0.5 h with 400 rpm, remained high until 1 h, and decreased slowly thereafter. The absorption capability due to the interfacial treatment is believed to increase, which leads to a decrease in the aligned movement of particles by the centrifugal force. On the other hand, the distribution depending on the particle size and better interfacial conditions had a significant effect on this pattern.

To understand these effects and produce a better FGM, it is necessary to develop a simple model. The FGM can be divided radically into many regions with an equal width with the same particle content, as shown in Figure 6. Figure 7 shows the compressive modulus as a function of the particle volume content (V_p).

If the compressive load is applied from the top of the specimen, a simple analytical model for the FGM can be derived as follows:

$$V_p = \sum_{i=1}^{n} V_i = \text{constant and } P_t = \sum_{i=1}^{n} P_i \tag{1}$$

The total volume of particles should be constant as a given percentage and the applied load should be distributed equally among the regions.

Because the displacement of this composite should be constant for all segments of the specimen under compression, the stress and strain relation gives

$$\frac{P_i h}{A_i E_i} = \text{constant} \tag{2}$$

where h and A are the height and area of each segment, and E_i is the compressive modulus of each segment. The total load can be represented as

$$P_t = P_1 \left(1 + \sum_{i=1}^{n} \frac{E_{i+1}}{E_1} \right) \tag{3}$$

where P_1 and E_1 are the load and modulus of the matrix ($V_p = 0$). Therefore, the modulus of FGM can be presented as

$$E_C = \frac{P_1}{k} \left(1 + \sum_{i=1}^{n} \frac{E_{i+1}}{E_1} \right) \text{ and } E_C \cong \sum_{i=1}^{n} \frac{E_{i+1}}{E_1} \tag{4}$$

where k is a constant.

Based on the experimental data of the particle-reinforced composite, the modulus of the composite increases in the following power fit with a particle volume fraction, [15,18] as shown in Figure 7.

Hence,

$$\frac{E_{ci}}{E_1} = \alpha e^{V_p \beta} + \gamma \tag{5}$$

The constant α, β and γ can be determined depending on the material types and properties. For the materials used in this study, they were $\alpha = 0.15$, $\beta = 8.35$ and $\gamma = 1.17$.

The compressive modulus is related directly to the sum of the segment modulus. Depending on the curve pattern, the load required to deform this FGM can be varied according to the distribution of particles in each segment. In general, the highest modulus was obtained with the stiffest outside layer with $V_p = 80$ or 100% of the given volume content. In addition, depending on the number of segments or particle size, the percentage of V_p in each segment should be changed. On the other hand, as V_p increases in the outside or in only one layer, the compressive modulus of FGM will increase. However, for the extreme case, excessive particles in the outside surface lead to pop out during the compressive loading; thus, the modulus decreases.

Figure 8 shows specific gravity profiles as function of distance from the specimen center with a normal curing process for RTV rubber by curing at room temperature. A curve for random represents the uniform distribution of silica throughout the specimen

without rotation. From the simple analytical concept, a curve for rotating at 560 rpm for 2 h can be the best reinforcing condition. However, the specimen of this curve normally has many silica particles at the surface of the specimen, which pop out during compressive loading. Therefore, it can have poor mechanical properties. As shown in Figures 3 and 4, the compressive modulus after a certain time of rotation depending on the particle size and volume decreases. The specimen with 100 μm and for 400 rpm * 1 h can be the best condition in this study. However, the best distribution profile can be determined based on the analytical model and should be determined as a function of the manufacturing conditions including the matrix and filler type. Based on those observations, it is believed that the ideal curve shown in Figure 8 will be the best condition for high compressive modulus. Similarly, Figure 9 shows the specific gravity profiles in the longitudinal direction to check the gravity effect during specimen preparation. A small gravity effect can be observed when the values of the top and bottom sides are compared. However, the values of the specific gravity of the specimen center and edge show a large difference in all cases.

If the specific gravity is proportional to the filler volume content, the filler volume distribution content with a transverse direction (Figure 8) can be generalized as follows:

$$V_p = ae^{br} \tag{6}$$

where r is the distance from the center to the surface of the specimen. In general, values of $a = 1.5–2$ and $b = 0.02–0.05$ can be obtained in a specimen with random or low gradient effects. In addition, values of $a = 0.05–0.1$ and $b = 0.2–0.4$ can be obtained in a specimen with high gradient effects. The optimal distribution pattern of particle in transverse direction can be obtained using Equations (5) and (6) at a given volume content. From these equations, the maximum gradient effects were found to be the specimen with the highest gradient distribution. On the other hand, the particles in the surface area with the highest gradient were unstable and popped out during compressive loading. Therefore, as shown in Figure 8, presented as the ideal curve, the optimized distribution pattern for a high compressive modulus is the high concentration

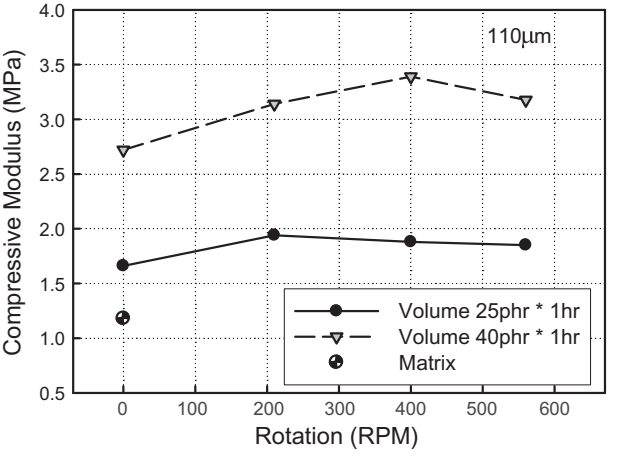

Figure 3. Effects of the RPM and volume content on the modulus of the composites.

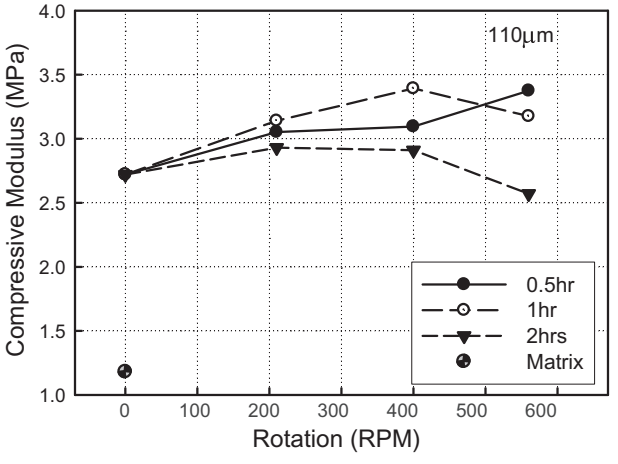

Figure 4. Effects of the RPM and rotation time on the modulus of reinforced composites.

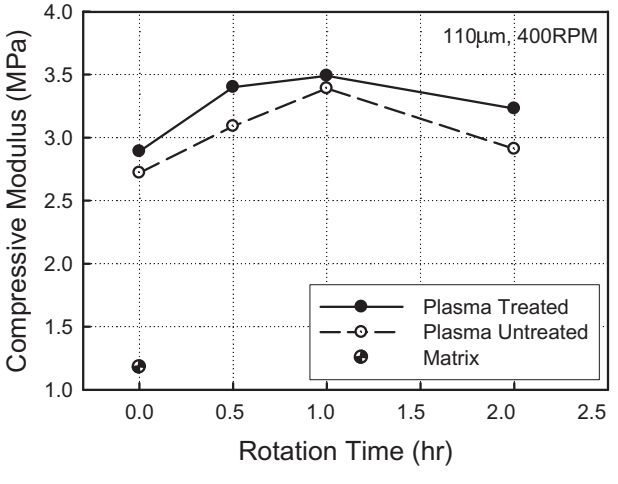

Figure 5. Effects of the plasma treatment and rotation time on the modulus of the reinforced composites.

in the localized area, in this case, the outside section, and the low concentration in the surface area to prevent the silica from popping out during compression.

To prevent the particle from locating extremely outside or from the surface with the highest gradient, it is necessary to cure fast in the surface area. In this study, this type of distribution pattern is obtained by the increase in surface temperature of mold during rotation from 30 to 75 °C for rapid curing at the mold surface. As shown in Figure 10, the compressive modulus increases differently with increasing temperature depending on the rotating time and then decreases at higher temperature. The figure suggests that the time for the optimal distribution of fillers depending on the curing speed can be predicted as a function of temperature at the mold surface. To check the compressive modulus changes as a function of curing temperature, the matrix is only

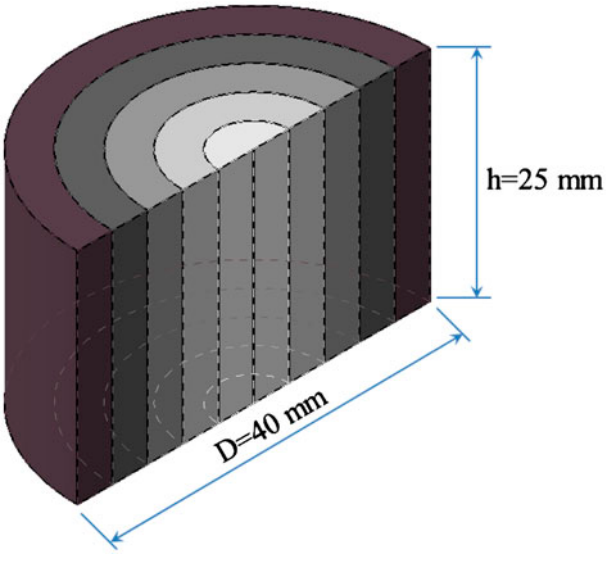

Figure 6. Schematic of FGM specimen.

cured from 20 to 78 °C, as shown in Figure 11. Even at low temperature around 35 °C, the compressive modulus decreases as the heating time at mold surface increases from 0.5 to 2 h. Since the silicone rubber used in this study was room temperature-cured silicone rubber, the compressive modulus decreased with increasing temperature. If the matrix is not degraded, it is believed that the non-uniform curing is caused. Therefore, the improvement of the compressive modulus, as shown in Figure 10, is only due to the filler distribution. And, it is found that the compressive modulus of the surface-cured specimen increased more than 40% compared to the regularly prepared FGM specimen without the surface heating shown in Figure 4. In addition, regardless of the rotation duration, the curing at the mold surface temperatures of 45–50 °C is the best condition for this rubber with 100 μm. This means that the fast curing near the mold surface and increasing of the viscosity slow the movement of the particle to outside of the mold. The temperature lower than 45 °C results in excessively slow curing and the temperature higher than 50 °C results in excessively fast curing, for the optimal distribution pattern of filler.

In addition, the specific gravity distribution with a transverse direction after 0.5 h at 38 and 46 °C was almost the same as before, as shown in Figure 12. This is not quite similar to the ideal curve shown in Figure 8. However, it is believed that this distribution pattern curve can be optimized, as shown in Figure 8, by adjusting the rotation time and surface temperature. In addition, the particle size and shape, and surface treatment are other factors in the manufacturing condition. If the matrix is not degraded or cured slowly, it is believed that the FGM with much better gradient effects can be obtained because the particle distribution can be arranged more drastically to achieve significantly improved properties. In general, if FGM develops distinctly different microstructures at different processing temperatures, it is possible to introduce property gradients by applying a temperature gradient during processing. It also needs a further study.

To understand the reinforcing mechanisms and to aid in design and fabrication processes involved in FGM, it is necessary to develop a simple model to explain this phenomenon. There have been many modeling studies to adequately describe the behavior and predict the performance of FGM.[16,19] However, many of these studies are limited to a certain condition such as thermo-physical properties or complex mathematical expression that needs many efforts and time to understand and apply to actual development.[17,20] Therefore, the simple model should be developed for various applications. Figure 13 shows the simplest schematic distribution pattern of the FGMs that contain the particle. If the geometric ratio between filled and unfilled regions is $R = r_c/r$, the degree of distribution gradient (D_g) can be generalized as $D_g = e^{(1-R)}$ based on two regions. In general, the experimental results of the compressive modulus vary with D_g according to the following equation:

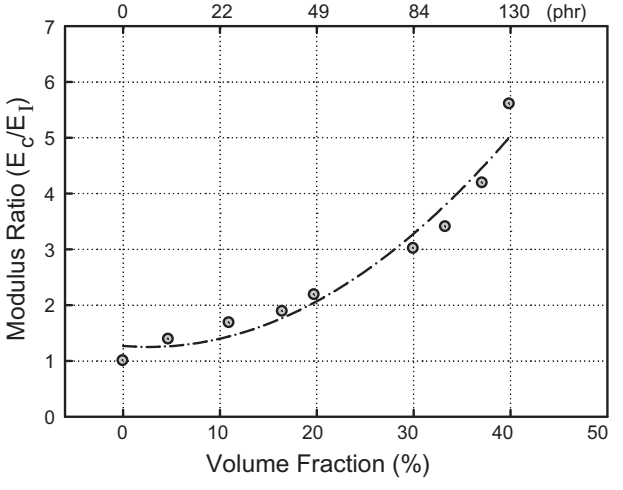

Figure 7. The compressive modulus ratio as a function of the particle volume content.

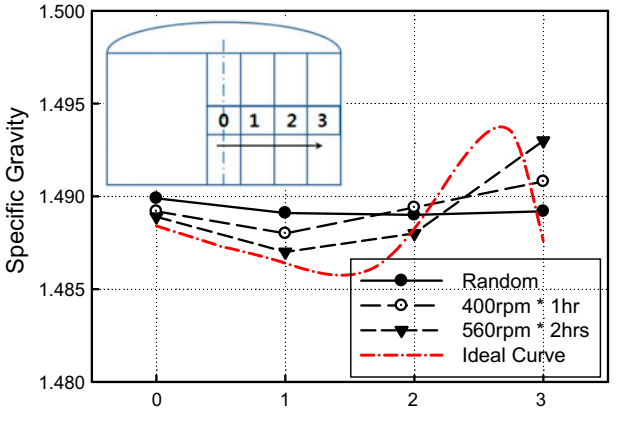

Figure 8. Specific gravity distribution with a transverse direction of the composites.

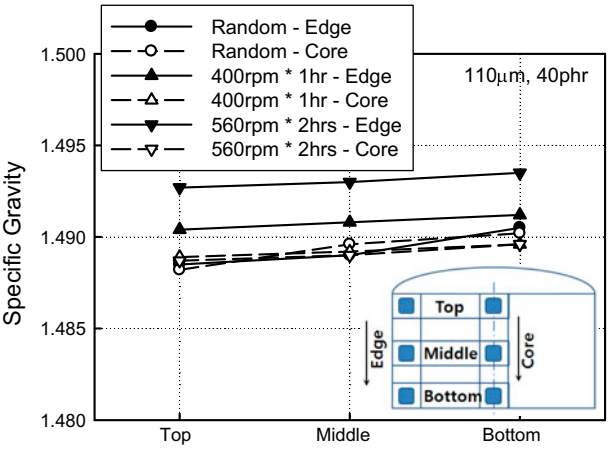

Figure 9. Specific gravity distribution with a longitudinal direction of the composites.

$$E_{\mathrm{FGM}} = D_g E_c \tag{7}$$

where E_{FGM} is the compressive modulus of FGM and E_c is the compressive modulus of the composite as a function of the filler content. If $R = 1$ as $r_c = r$, then D_g will be 1 and E_{FGM} will be a composite with a uniform distribution throughout the specimen at a given filler content, and $E_{\mathrm{FGM}} = E_c$. Therefore, degree of the distribution gradient (D_g) should be maximized to have the best compressive properties. As expected, a higher D_g could be obtained by increasing the rotating speed and time. Because E_c is

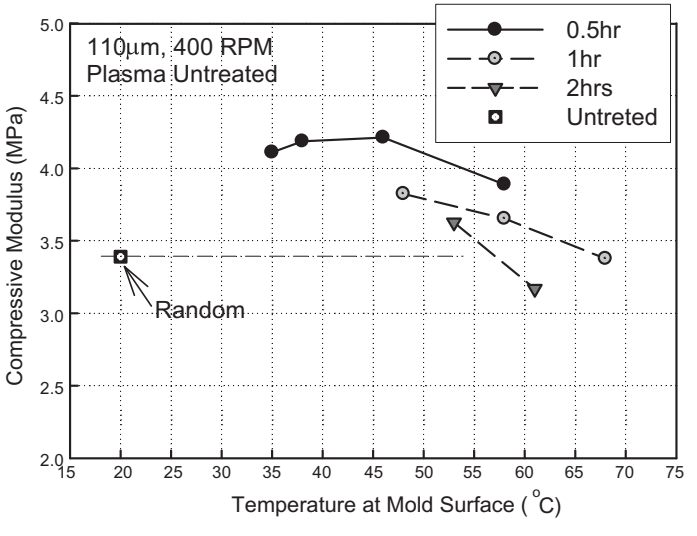

Figure 10. Compressive modulus after 0.5, 1, and 2 h of rotation at 400 rpm as a function of the curing temperature at the mold surface for 110 μm silica.

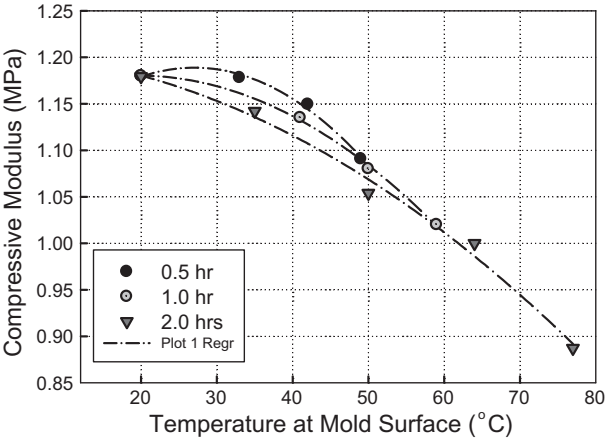

Figure 11. Compressive modulus of the matrix as a function of the temperature at the mold surface.

generalized from Figure 7 as $E_c = E_m(1.5e^{8.35V_c} + 1.17)$ as a function of particle content, the compressive modulus of FGM is defined as

$$E_{\mathrm{FGM}}/E_m = e^{(1-R)}(1.5e^{8.35V_c} + 1.17) \tag{8}$$

Figure 14 shows the model-predicted modulus ratio as a function of R, D_g, and V_p. Considering the specimen with a given D_g and filler content, the compressive modulus can be obtained for different types of the matrix because the ratio of the compressive modulus of different rubbers is similar for particles or short fiber-reinforced rubber, as predicted by the Halpin–Tsai equation.[18]

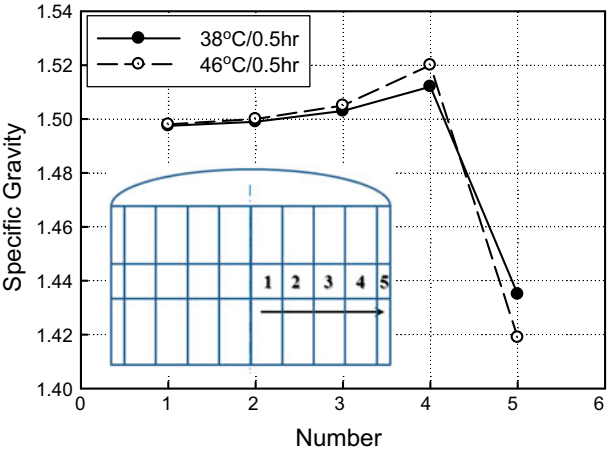

Figure 12. Specific gravity distribution with a transverse direction after 0.5 h at 38 °C and 46 °C.

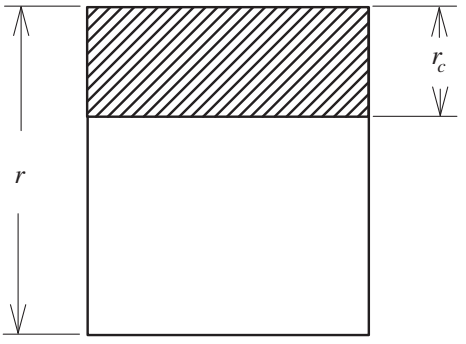

Figure 13. Schematic distribution pattern of the FGMs that contain the particle.

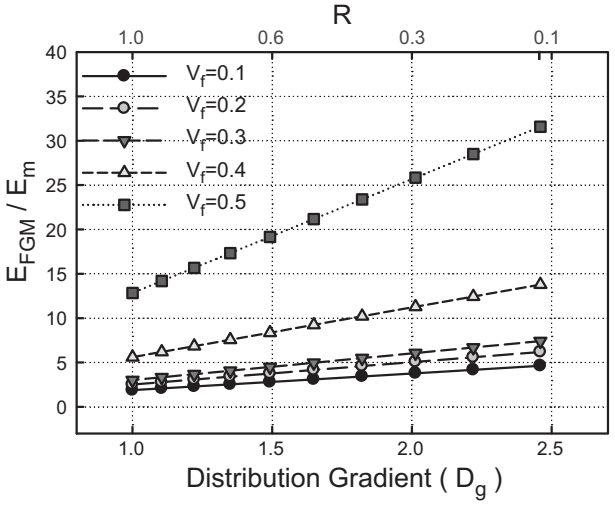

Figure 14. The model-predicted modulus ratio shown as a function of D_g and V_p.

Therefore, this type of simple model can be used as a guideline for manufacturing and to better understand the reinforcing mechanisms of FGMs. In this case, as the volume content of filler increases, the effect of D_g on compressive properties is more significant. To make it more realistic to a real FGM composite, it is necessary to expand D_g to various degrees considering the probability distribution pattern for the particle size. In addition, other factors, such as the content and distribution, which affect the mechanical properties of FGMs depending on the loading condition, matrix properties, and filler type, should be considered. Although the change in particle size and shape used in this study was not investigated, the size and shape variation are also important factors for a range of properties, particularly for the dynamic properties. However, the expansion of this model will be published in another paper with the dynamic properties of this FGM introduced, because the dynamic properties related to the performance of the damper and absorber is related directly to the modulus. Those will be discussed in the later paper.

In general, a graded particle distribution has a beneficial impact on the modulus. If modeled and fabricated well, the optimized FGM can be valuable, such as reduced

weight, maximized loading carrying capability and fracture resistance, and optimized heat transfer or insulation.

4. Conclusions

The compressive properties of silica-reinforced FGM that fabricated by the centrifugal method was studied depending on the silica particle size and V_p. In addition, the effects of the interfacial treatment were discussed. As expected, the particle size, the rotating time, and speed have significant influences on the gradient effects. On the other hand, there is window of manufacturing processes for the optimal distribution pattern in the specimen. A simple analytical model was developed to understand these phenomena, which can also act as a guideline for manufacturing better FGM composites. In general, the degree of the distribution gradient (D_g) should be maximized to have the best compressive properties. A higher D_g could be obtained by increasing the rotating speed and time. Although it is difficult to make a FGM as predicted, the optimal FGM can be pursued. Experimentally, the compressive modulus of FGM increases more than 40% up to 64% compared to the randomly oriented specimen.

Surface treatments of silica significantly affect the manufacturing conditions due to a higher adsorption capacity of rubber molecules that interfere with the silica movement by the centrifugal force. These can reduce the processing time and increase the mechanical properties significantly.

Acknowledgements

This study was supported by the Research Grant from Yeungnam University in 2012.

References

[1] Morton M. Liquid 1,2-vinyl polybutadienes and modified polybutadienes as resin matrix in laminates, rubber technology. 2nd ed. New York (NY): Van Nostrand Reinhold Co.; 1973.
[2] Prasertsri S, Rattanasom N. Mechanical and damping properties of silica/natural rubber composites prepared from latex system. Polym. Test. 2011;30:515–526.
[3] Ciesielski A. An introduction to rubber technology. Shrewsbury: Rapra Technology Ltd. 1999:184.
[4] He Z, Ma J, Tan GEB. Fabrication and characteristics of alumina–iron functionally graded materials. J. Alloys Compd. 2009;486:815–818.
[5] Ryu SR, Lee DJ. Effects of short-fiber shape on tensile properties of reinforced rubber. J. Mat. Sci. 2007;42:1019–1025.
[6] Ryu SR, Lee DJ. Effects of interphase and short fiber on puncture and burst properties of short-fiber reinforced chloroprene rubber. J. Elastomers Plast. 2010;42(2):181–197.
[7] Tsotra P, Friedrich K. Electrical and mechanical properties of functionally graded epoxy-resin/carbon fibre composites. Composites Part A. 2003;34:75–82.
[8] Watanabe Y, Kawamoto A, Matsuda K. Particle size distribution in functionally graded materials fabricated by centrifugal solid-particle method. Compos. Sci. Technol. 2002;62: 881–888.
[9] Hashmi SAR, Dwivedi UK. SiC dispersed polysulphide epoxy resin based functionally graded material. Polym. Compos. 2009;30:162–168.
[10] Krumova M, Klingshirn C, Haupert F, Friedrich K. Microhardness studies on functionally graded polymer composites. Compos. Sci. Technol. 2001;61:557–563.
[11] Kirugulige MS, Tippur HV. Mixed-mode dynamic crack growth in functionally graded glass-filled epoxy. Exp. Mech. 2006;46:269–281.
[12] Liu XQ, Wang YS, Zhu JH. Epoxy resin/polyurethane functionally graded material prepared by microwave irradiation. J. Appl. Polym. Sci. 2004;94:994–999.

[13] Leblanc JL. Rubber-filler interactions and rheological properties in filled compounds. Prog. Polym. Sci. 2002;27:627–687.
[14] Tomozawa M, Kim DL, Lou V. Preparation of high purity, low water content fused silica glass. J. Non-Cryst. Solids. 2001;296:102–106.
[15] Subramaniyan AK, Sun CT. Enhancing compressive strength of unidirectional polymeric composites using nanoclay. Composites Part A. 2006;37:2257–2268.
[16] Markworth AJ, Ramesh KS, Parks WP. Modelling studies applied to functionally graded materials. J. Mat. Sci. 1995;30:2183–2193.
[17] Pascon JP, Coda HB. High-order tetrahedral finite elements applied to large deformation analysis of functionally graded rubber-like materials. Appl. Math. Model. 2013;37: 8757–8775.
[18] Gibson RF. Principles of Composite Material Mechanics. New York (NY): McGraw-Hill Inc; 1994.
[19] Kieback B, Neubrand A, Riedel H. Processing techniques for functionally graded materials. Mat. Sci. Eng. A. 2003;A362:81–106.
[20] Torquato S. Random heterogeneous materials: Microstructure and macroscopic properties. New York (NY): Springer-Verlag; 2002.